

Structure of C3b reveals conformational changes that underlie complement activity

Bert J. C. Janssen¹, Agni Christodoulidou², Andrew McCarthy³, John D. Lambris² & Piet Gros¹

Resistance to infection and clearance of cell debris in mammals depend on the activation of the complement system, which is an important component of innate and adaptive immunity^{1,2}. Central to the complement system is the activated form of C3, called C3b, which attaches covalently to target surfaces³ to amplify complement response, label cells for phagocytosis and stimulate the adaptive immune response. C3b consists of 1,560 amino-acid residues and has 12 domains. It binds various proteins and receptors to effect its functions⁴. However, it is not known how C3 changes its conformation into C3b and thereby exposes its many binding sites. Here we present the crystal structure at 4-Å resolution of the activated complement protein C3b and describe the conformational rearrangements of the 12 domains that take place upon proteolytic activation. In the activated form the thioester is fully exposed for covalent attachment to target surfaces and is more than 85 Å away from the buried site in native C3 (ref. 5). Marked domain rearrangements in the α -chain present an altered molecular surface, exposing hidden and cryptic sites that are consistent with known putative binding sites of factor B and several complement regulators. The structural data indicate that the large conformational changes in the proteolytic activation and regulation of C3 take place mainly in the first conversion step, from C3 to C3b. These insights are important for the development of strategies to treat immune disorders that involve complement-mediated inflammation.

The complement system is important for host defence in metazoans¹. In mammals, complement provides an essential link between innate and adaptive immunity². The complement system has also been proposed to be involved in tissue regeneration, neuron development, wound healing and reproduction⁶, indicating that it has a broad role in cell differentiation. The system consists of about 35 cell-surface and soluble plasma proteins. Cleavage of C3 (186 kDa) into C3b (177 kDa) and C3a (9 kDa) is the central step in the complement activation cascade, which can be initiated by three different pathways—the classical, lectin and alternative pathways. C3b covalently attaches to pathogenic, or apoptotic, target surfaces through its reactive thioester moiety⁷ and thereby induces several biological processes. C3b provides a molecular platform for the formation of convertase complexes. Binding of pro-enzyme factor B to C3b and subsequent cleavage of factor B by factor D yields the short-lived ($t_{1/2} \approx 90$ s) C3bBb complex⁸, which converts C3 into C3b and C3a, thereby amplifying the complement response and forming the C3b₂Bb complex that cleaves C5 to initiate the formation of large, membrane-inserted lytic pores. In addition, deposition of C3b on target surfaces generates two important cellular responses. C3b and its proteolytic fragments iC3b and C3dg (Fig. 1) are recognized by complement receptors (CR) on phagocytic cells (for example, CR1 (CD35), CR3 (CD11b/CD18), CR4 (CD11c/CD18)² and CRIg⁹) to induce the

uptake of opsonized particles, and by CR2 (CD35) to upregulate the B-cell response 10,000-fold through the co-stimulatory and B-cell receptor complexes¹⁰. The formation of C3b is therefore a crucial step that requires tight regulation. Host cells express several cell-surface and soluble regulators that disrupt the C3bBb complex or aid in the proteolytic degradation of C3b into iC3b and ultimately to C3dg and C3c^{11,12}. Bacteria and viruses use proteins with similar activities to evade the complement response. Because C3b binds many soluble proteins and cell-surface receptors⁴, whereas C3 has few binding partners, the proteolytic activation of C3 into C3b probably induces conformational changes that form the various cryptic binding sites. Conformation-dependent mechanisms are probably common to the homologous proteins of the C3/ α 2-macroglobulin family, which are an ancient family of host defence proteins.

Here we present the crystal structure of human C3b solved at 4-Å resolution by molecular replacement using the structures of C3, C3c⁵ and C3d¹³; see Methods and Supplementary Table 1 and Supplementary Fig. 1. C3b is generated from C3 by proteolytic removal of the small anaphylatoxin domain (residues 650–726) to produce a β -chain (residues 1–645) and a shortened α -chain, denoted α' (residues 727–1,641). The structure of C3b reveals that this conversion is accompanied by marked structural rearrangements that result in differences in atomic position of up to 95 Å (Fig. 1). The domain rearrangements can be described by a metaphor of a puppeteer with a body formed by the β -ring domains (macroglobulin (MG) 1–6 domains and linker (LNK) domain), shoulders (domains MG7 and MG8), a neck (anchor region), a head (C345C domain) and an arm ('complement C1r/C1s, Uegf, Bmp1' (CUB) domain) with a puppet (thioester-containing domain (TED)). In C3 the puppet (TED domain) is embraced by the arm (CUB) and held against the shoulder (MG8). In C3b the shoulders (MG7 and MG8), neck (anchor) and head (C345C) have twisted, the arm (CUB) has extended downwards and the puppet (TED) has dropped (see Supplementary Table 2 and Movie 1). In its new position, the TED domain contacts MG1 of the β -ring. The single amino-acid residue difference, Arg80Gly in MG1, that is responsible for the C3S/C3F phenotype difference¹⁴ is located in the MG1–TED interface. The overall arrangement of the core domains (MG1–8, LNK, anchor and C345C) resembles more the structural arrangement of the final proteolytic, downregulated fragment C3c than the native C3 molecule. This includes the relocation of the α' amino-terminal segment (α' NT) and the conformational transition of the MG8 $\beta\alpha\beta$ -motif in C3 to a $\beta\alpha\alpha$ -motif in C3b and C3c. The TED domain (which is absent in C3c) takes on the conformation that is seen in the C3d fragment¹³. Thus, in the proteolytic conversion of C3 to C3b, iC3b and finally C3c and C3dg, the main conformational rearrangements occur upon the first activation step that converts the native, resting C3 into the active C3b.

¹Crystal and Structural Chemistry, Bijvoet Center for Biomolecular Research, Faculty of Sciences, Utrecht University, Padualaan 8, 3584 CH Utrecht, The Netherlands. ²Department of Pathology and Laboratory Medicine, School of Medicine, University of Pennsylvania, Philadelphia 19104, USA. ³European Molecular Biology Laboratory, Grenoble Outstation, 38042 Grenoble, Cedex 9, France.

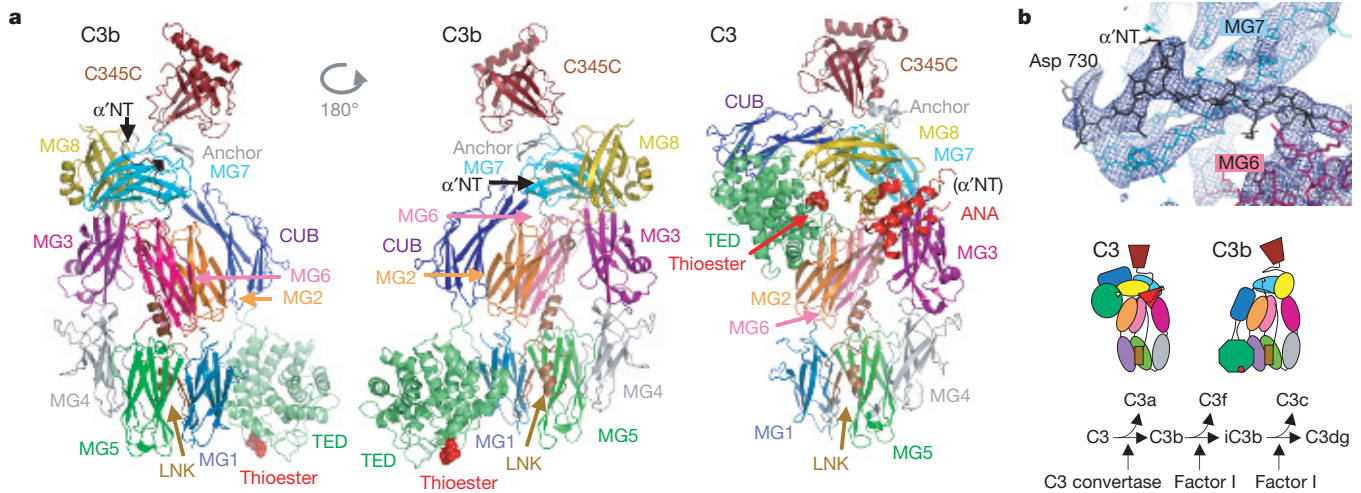


Figure 1 | Structure of C3b at 4-Å resolution. **a**, Ribbon representation in two views of C3b coloured by domain and labelled accordingly. Also indicated are the exposed thioester moiety (red spheres), anchor region (grey) and α' NT (black). For comparison, the ribbon representation of C3 and cartoons of the domain arrangements in C3b and C3 are added. **b**, Electron density ($2mF_{obs} - DF_{calc}$ ϕ_{calc}) contoured at 1σ of the α' NT region with domains as indicated; density maps for each domain are given in Supplementary Fig. 1. The proteolytic steps of C3 conversion are shown schematically.

Surface attachment of C3b requires exposure and activation of the thioester moiety, Cys 988–Gln 991 of the TED domain. In the structure of C3b these residues are completely exposed to the solvent, whereas in C3 they are hidden⁵ 85 Å away from the site of exposure. In addition, the TED domain in C3b has changed its conformation from C3-like⁵ to C3d-like¹³, where the arrangement of the reactive residues corresponds to the formation of the acyl-imidazole intermediate, which is highly reactive towards hydroxyl nucleophiles^{5,15} (Fig. 2a). The overall domain rearrangements might be coupled to the conformational changes in the TED domain by a pulling force that stretches the N-terminal segment (helices $\alpha 0$ and $\alpha 1$) preceding the thioester cysteine. Surface-charge calculation shows a single, strong electro-positive patch near the thioester, on a protein that is

otherwise mostly and strongly electro-negative (Fig. 2b). Putatively, the electropositive patch on the TED domain is involved in orienting the molecule with respect to negatively charged target surfaces, such as bacterial cells or apoptotic host cells. This orientation results in a footprint of $50 \times 90 \text{ \AA}^2$ formed by the TED, MG1, MG4 and MG5 domains, which is in remarkable agreement with the figure of $\sim 4,750 \text{ \AA}^2$ that was estimated from fully covered erythrocytes¹⁶. Proper orientation of the TED domain close to the target surface might be important for the highly reactive and short-lived ($t_{1/2} < 100 \mu\text{s}$)¹⁷ acyl-imidazole intermediate to react covalently with the target surface instead of the surrounding solvent.

Conversion of C3 to C3b exposes binding sites for proteins involved in convertase formation (factor B and properdin) and

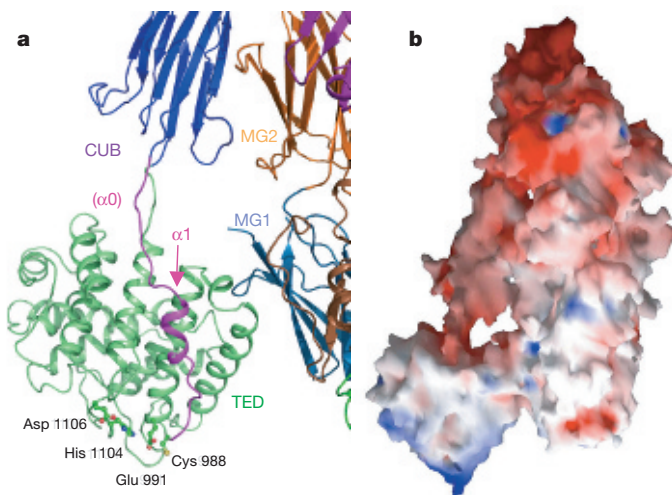


Figure 2 | Thioester exposure for covalent target attachment. **a**, Ribbon representation of the TED domain with the exposed thioester moiety; residues of the acyl-intermediate are shown in ball-and-stick. Indicated in magenta are the regions corresponding to $\alpha 0$ and $\alpha 1$ in C3, which are displaced from the TED domain in C3b. **b**, Surface charge representation³⁰ (shown between -12 (red) and $+12$ kT (blue)) of C3b indicating the overall negative surface-charge potential and the positive patch around the thioester moiety on the TED domain.

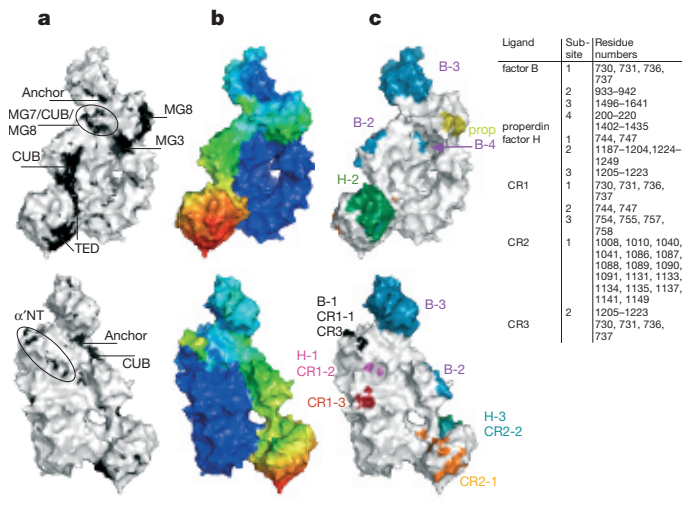


Figure 3 | Exposure and generation of cryptic binding sites. **a**, Surface representation of C3b indicating regions exposed in C3b but hidden in C3 (black). **b**, Novel surface arrangements indicated by conformational change (from C3 to C3b) mapped onto the molecular surface, rainbow colouring from minimum (0 Å; blue) to maximum (95 Å; red) coordinate change. **c**, Mapping of the putative binding sites for factor B, properdin, factor H, CR1, CR2 and CR3 as indicated (references as given in the text). Lower panels are rotated 130° relative to upper panels; surface calculated by rolling a sphere of 4-Å radius.

dissociation (regulators of complement). We analysed the C3b surface for exposure of previously hidden interfaces and for new arrangements of sites already exposed on C3 (Fig. 3a, b). The new N-terminal segment α' NT (residues 727–745) carries four acidic residues that are important for binding factor B. Previously we have shown that this segment undergoes a drastic relocation between the native C3 and the final proteolytic fragment C3c (ref. 5). The structure of C3b reveals that this relocation, in which the α' NT moves through the central hole of the β -ring and becomes exposed on the opposite side of the molecule, occurs during the activation of C3 into C3b. Mapping other putative binding sites for factor B onto the C3b surface (Fig. 3c) gives three exposed sub-sites, α' NT¹⁸, strand β 4 of CUB¹⁹ and C345C²⁰ (whereas the putative 'complement C2 receptor inhibitor trispanning' (CRIT) like site²¹ remains mostly occluded), that are located around the shoulder (MG7), neck and head region. This region undergoes significant structural rearrangements from C3 to C3b (Fig. 2b). The absence of novel features on the surface of the β -ring excludes this region as a primary binding site of factor B. In addition, the TED domain is probably not a primary binding site for factor B, because cobra-venom factor, which is a C3b homologue that can make potent fluid-phase convertases, lacks a TED domain.

The association of C3b and factor B is accelerated by properdin, which also stabilizes the resulting convertase C3bBb. The putative binding site of properdin has been mapped to residues 1402–1435 (ref. 22), which form the structurally variable $\beta\alpha\beta$ - $\beta\alpha\alpha$ motif in the MG8 domain. This site is hidden in C3 and becomes exposed in C3b (Fig. 3a). Thus, the arrangement of putative binding sites identifies the arm-shoulder-neck-head region as being responsible for binding factor B and properdin. Regulators of complement (including soluble factor H and cell-surface CR1 and decay-accelerating factor (DAF/CD55)) dissociate the C3bBb complex and act as co-factors in the proteolysis of C3b into iC3b (for example, factor H, CR1 and cell-surface membrane-cofactor protein (MCP/CD46)). Three regions have been implicated in regulator binding: the α' NT (for factor H and CR1), the MG6 domain (for factor H and CR1)²³ and the TED domain (for factor H)²⁴. In the structure of C3b, α' NT and MG6 form one continuous exposed region, indicating that the binding site for factor B overlaps with that for factor H and CR1. Therefore, dissociation of C3bBb by these regulators is achieved through steric hindrance. Binding of factor H to the TED domain might be linked to its cofactor activity. Protease factor I, which degrades C3b by three sequential cleavages (see Supplementary Fig. 2), requires these cofactors (for example, factor H, CR1 or MCP), putatively for orienting its protease domain and unraveling the CUB domain. The resulting iC3b no longer binds factor B. As the arrangement of the 10 domains in C3c is similar to that in C3b, it is likely that iC3b has the same overall core-domain arrangement. Therefore, it seems that the stability of the convertase depends on the structure and orientation of the CUB domain with respect to the rest of C3b.

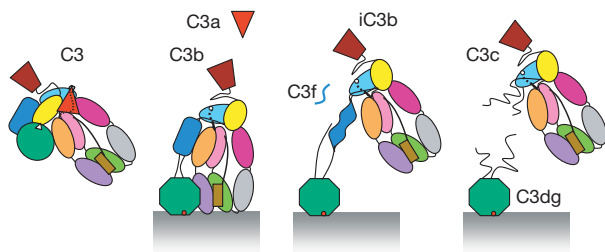


Figure 4 | Proposed model for the conformational pathway of C3. Shown schematically are the four stages: C3, C3b with C3a, iC3b with C3f and C3dg with C3c (see also Supplementary Fig. 2). These conformational changes determine the binding affinities towards soluble proteins (for example, factor B, properdin and factor H) and cell-surface receptors (for example, CR1–4, CRiG, DAF and MCP) that underlie the biological activity.

C3b, iC3b and C3dg induce various cellular responses. C3b and iC3b act as opsonins to facilitate the uptake of tagged particles. This occurs through specific recognition of C3b and iC3b by complement receptors on various phagocytic cells². C3b is recognized by CR1 and CRiG⁹ whereas iC3b is also recognized by the integrins CR3 and CR4. Furthermore, pathogen-bound iC3b and C3dg, but not C3b, contribute to an increased antibody response by binding to CR2 on B cells. A putative binding site for CR2 has been mapped partly on the interface between the TED and MG1 domains²⁵, close to the TED–CUB connections. Therefore it seems likely that, when the TED–CUB connections in iC3b are disrupted, the TED–MG1 interface is opened to provide a new interface for binding CR2 on B cells. Dislodging the iC3b core from the TED domain and the target surface might provide the new signal for binding the integrins CR3 and CR4 on phagocytic cells.

In summary, these data indicate a conformational pathway for C3 and its fragments (Fig. 4) that determines their biological activity. In this pathway, the β -ring provides a stable platform for the functionally important domains of the α -chain that undergo conformational rearrangements. We expect that similar rearrangements occur in homologous host-defence proteins (see Supplementary Fig. 3, where we modelled native α 2-macroglobulin and activated α 2-macroglobulin in electron-microscopy reconstruction maps). Insights into these marked conformational changes are essential for understanding convertase activity and regulation, and will help in the development of complement inhibitors for therapeutic use.

METHODS

Protein purification. C3 was isolated from citrated human plasma as previously described²⁶ with the exception that after the diethylaminoethyl (DEAE) column it was converted to C3b by limited digestion with trypsin for 2 min at 37 °C with 1% w/w enzyme/substrate (the reaction was stopped by the addition of 3% w/w soybean trypsin inhibitor). The C3b was purified immediately by gel filtration over a Superdex 200 size-exclusion column in phosphate buffered saline pH 7.4, followed by anion-exchange chromatography over a Mono-Q column (equilibrated in 50 mM phosphate buffer, pH 7.5 and eluted with 20 column volumes of 0–500 mM NaCl gradient). The protein was then treated with 100 mM iodoacetamide (30 min at 4 °C) to prevent dimerization of the C3b by the free cysteine, concentrated and further purified over a Mono-S column equilibrated in 50 mM phosphate buffer pH 6.0 and eluted with 20 column volumes of 0–500 mM NaCl gradient. The C3b was concentrated to 10 mg ml⁻¹, dialysed against 10 mM Tris pH 7.4 and frozen at –70 °C until crystallization.

Crystallization and crystallography. C3b was crystallized in sitting drops from mother liquor containing 9% w/v PEG-monomethylether 2000, 100 mM sodium acetate, 10 mM taurine and 50 mM Bis-Tris propane pH 7.8 at 30 °C. Crystals grew to 100 × 100 × 60 μ m within 2 weeks. For cryo-protection, the well solution was replaced by mother liquor with increased (to 40% w/v) PEG-monomethylether 2000 and equilibrated for 24 h at 30 °C; and crystals were flash-cooled in liquid nitrogen. Crystals displayed space group $P2_12_12$ ($a = 123.9$, $b = 128.5$, $c = 147.0$ Å), contained one molecule per asymmetric unit and diffracted to 4-Å resolution at ESRF beamline ID14-EH4. Diffraction data was processed using MOSFLM/CCP4 (ref. 27) (data statistics are presented in Supplementary Table 1).

Structure determination. C3b was solved by molecular replacement with Phaser²⁸. First, the MG1–MG6 and LNK domains of C3c (pdb code 2A74)⁵ were placed. Second, we placed C3d (pdb code 1C3D)¹³, yielding a large log-likelihood gain (see Supplementary Table 1B) as compared with a loss of log-likelihood when testing the TED domain from C3 (pdb code 2A73)⁵. Finally, we added step-by-step MG8, MG7, α' NT, anchor and C345C from C3c and CUB from C3, respectively, using molecular graphics in Coot²⁹ with rigid-body refinement in Phaser. This yielded a 97% complete model that was completed by model building of the CUB–TED connections (17 residues) and slight adjustments in the other domain–domain connections. Owing to limited resolution only one round of restrained refinement followed by one round of 'translation, liberation and screw-rotation' (TLS) refinement (with individual B-factors set to 50 Å²) were performed in REFMAC²⁷. The final refined model of C3b, consisting of 1,531 residues, had R and R_{free} values of 27.3 and 32.3%, respectively (for model statistics see Supplementary Table 1). Electron density for each domain is shown in Supplementary Fig. 1; see also Fig. 1b. The central domains fitted excellently in the electron density; the outermost domains (CUB, TED and C345C) showed

convincing, but weaker, electron density. All molecular graphics figures, except Fig. 2b, were generated with pymol (W. Delano; <http://www.pymol.org/>).

Received 9 July; accepted 15 August 2006.

Published online 15 October 2006.

- Walport, M. J. Complement. First of two parts. *N. Engl. J. Med.* **344**, 1058–1066 (2001).
- Carroll, M. C. The complement system in regulation of adaptive immunity. *Nature Immunol.* **5**, 981–986 (2004).
- Law, S. K. & Levine, R. P. Interaction between the third complement protein and cell surface macromolecules. *Proc. Natl Acad. Sci. USA* **74**, 2701–2705 (1977).
- Lambris, J. D. The multifunctional role of C3, the third component of complement. *Immunol. Today* **9**, 387–393 (1988).
- Janssen, B. J. *et al.* Structures of complement component C3 provide insights into the function and evolution of immunity. *Nature* **437**, 505–511 (2005).
- Mastellos, D. & Lambris, J. D. Complement: more than a 'guard' against invading pathogens? *Trends Immunol.* **23**, 485–491 (2002).
- Tack, B. F., Harrison, R. A., Janatova, J., Thomas, M. L. & Prah, J. W. Evidence for presence of an internal thioester bond in third component of human complement. *Proc. Natl Acad. Sci. USA* **77**, 5764–5768 (1980).
- Fishelson, Z., Pangburn, M. K. & Muller-Eberhard, H. J. Characterization of the initial C3 convertase of the alternative pathway of human complement. *J. Immunol.* **132**, 1430–1434 (1984).
- Helmy, K. Y. *et al.* CRlg: a macrophage complement receptor required for phagocytosis of circulating pathogens. *Cell* **124**, 915–927 (2006).
- Dempsey, P. W., Allison, M. E., Akkaraju, S., Goodnow, C. C. & Fearon, D. T. C3d of complement as a molecular adjuvant: bridging innate and acquired immunity. *Science* **271**, 348–350 (1996).
- Ross, G. D., Lambris, J. D., Cain, J. A. & Newman, S. L. Generation of three different fragments of bound C3 with purified factor I or serum. I. Requirements for factor H vs CR1 cofactor activity. *J. Immunol.* **129**, 2051–2060 (1982).
- Harrison, R. A. & Lachmann, P. J. Novel cleavage products of the third component of human complement. *Mol. Immunol.* **17**, 219–228 (1980).
- Nagar, B., Jones, R. G., Diefenbach, R. J., Isenman, D. E. & Rini, J. M. X-ray crystal structure of C3d: a C3 fragment and ligand for complement receptor 2. *Science* **280**, 1277–1281 (1998).
- Brown, K. M. *et al.* Influence of donor C3 allotype on late renal-transplantation outcome. *N. Engl. J. Med.* **354**, 2014–2023 (2006).
- Dodds, A. W., Ren, X. D., Willis, A. C. & Law, S. K. The reaction mechanism of the internal thioester in the human complement component C4. *Nature* **379**, 177–179 (1996).
- Pangburn, M. K., Schreiber, R. D. & Muller-Eberhard, H. J. C3b deposition during activation of the alternative complement pathway and the effect of deposition on the activating surface. *J. Immunol.* **131**, 1930–1935 (1983).
- Sim, R. B., Twose, T. M., Paterson, D. S. & Sim, E. The covalent-binding reaction of complement component C3. *Biochem. J.* **193**, 115–127 (1981).
- Taniguchi-Sidle, A. & Isenman, D. E. Interactions of human complement component C3 with factor B and with complement receptors type 1 (CR1, CD35) and type 3 (CR3, CD11b/CD18) involve an acidic sequence at the N-terminus of C3 alpha'-chain. *J. Immunol.* **153**, 5285–5302 (1994).
- O'Keefe, M. C., Caporale, L. H. & Vogel, C. W. A novel cleavage product of human complement component C3 with structural and functional properties of cobra venom factor. *J. Biol. Chem.* **263**, 12690–12697 (1988).
- Kolln, J., Spillner, E., Andra, J., Klensang, K. & Bredehorst, R. Complement inactivation by recombinant human C3 derivatives. *J. Immunol.* **173**, 5540–5545 (2004).
- Inal, J. M. & Schifferli, J. A. Complement C2 receptor inhibitor trispanning and the beta-chain of C4 share a binding site for complement C2. *J. Immunol.* **168**, 5213–5221 (2002).
- Daoudaki, M. E., Becherer, J. D. & Lambris, J. D. A 34-amino acid peptide of the third component of complement mediates properdin binding. *J. Immunol.* **140**, 1577–1580 (1988).
- Oran, A. E. & Isenman, D. E. Identification of residues within the 727–767 segment of human complement component C3 important for its interaction with factor H and with complement receptor 1 (CR1, CD35). *J. Biol. Chem.* **274**, 5120–5130 (1999).
- Lambris, J. D., Avila, D., Becherer, J. D. & Muller-Eberhard, H. J. A discontinuous factor H binding site in the third component of complement as delineated by synthetic peptides. *J. Biol. Chem.* **263**, 12147–12150 (1988).
- Clemenza, L. & Isenman, D. E. Structure-guided identification of C3d residues essential for its binding to complement receptor 2 (CD21). *J. Immunol.* **165**, 3839–3848 (2000).
- Lambris, J. D., Dobson, N. J. & Ross, G. D. Release of endogenous C3b inactivator from lymphocytes in response to triggering membrane receptors for beta 1H globulin. *J. Exp. Med.* **152**, 1625–1644 (1980).
- The C. C. P. 4 suite: programs for protein crystallography. *Acta Crystallogr. D Biol. Crystallogr.* **50**, 760–763 (1994).
- Storoni, L. C., McCoy, A. J. & Read, R. J. Likelihood-enhanced fast rotation functions. *Acta Crystallogr. D Biol. Crystallogr.* **60**, 432–438 (2004).
- Emsley, P. & Cowtan, K. Coot: model-building tools for molecular graphics. *Acta Crystallogr. D Biol. Crystallogr.* **60**, 2126–2132 (2004).
- Nicholls, A., Bharadwaj, R. & Honig, B. GRASP: Graphical representation and analysis of surface properties. *Biophys. J.* **64**, 166–170 (1993).

Supplementary Information is linked to the online version of the paper at www.nature.com/nature.

Acknowledgements We acknowledge the European Synchrotron Radiation Facility for provision of synchrotron radiation facilities; and S.J. Kolodziej and J.K. Stoops (Houston) for providing the native α 2-macroglobulin and methylamine-treated α 2-macroglobulin EM-reconstruction maps. We thank B. Nilsson (Uppsala), R.B.G. Ravelli (Grenoble) and E.G. Huizinga (Utrecht) for reading the manuscript. This work was supported by a 'Pioneer' programme grant to P.G. by the Council for Chemical Sciences of the Netherlands Organization for Scientific Research (NWO-CW) and an NIH grant to J.D.L.

Author Information Coordinates and structure factors of the C3b structure have been deposited in the Protein Data Bank with accession number 2I07. Reprints and permissions information is available at www.nature.com/reprints. The authors declare no competing financial interests. Correspondence and requests for materials should be addressed to P.G. (p.gros@chem.uu.nl).